Quantum State Tomography via Reduced Density Matrices

Tao Xin, Dawei Lu, Joel Klassen, Nengkun Yu, Zhengfeng Ji, Jianxin Chen, Xian Ma, Guilu Long, Bei Zeng, and Raymond Laflamme

Phys. Rev. Lett. **118**, 020401 — Published 9 January 2017

DOI: 10.1103/PhysRevLett.118.020401

Quantum state tomography via reduced density matrices

Tao Xin,[1,2] Dawei Lu,[2] Joel Klassen,[2,3] Nengkun Yu,[2,4,5,*] Zhengfeng Ji,[4,6] Jianxin Chen,[7] Xian Ma,[2,8] Guilu Long,[1] Bei Zeng,[2,5,9,†] and Raymond Laflamme[2,9,10]

[1]*State Key Laboratory of Low-Dimensional Quantum Physics and Department of Physics, Tsinghua University, Beijing 100084, China*
[2]*Institute for Quantum Computing, University of Waterloo, Waterloo N2L 3G1, Ontario, Canada*
[3]*Department of Physics, University of Guelph, Guelph, Ontario, Canada*
[4]*Centre for Quantum Computation & Intelligent Systems, Faculty of Engineering and Information Technology, University of Technology Sydney, NSW 2007, Australia*
[5]*Department of Mathematics & Statistics, University of Guelph, Guelph, Ontario, Canada*
[6]*State Key Laboratory of Computer Science, Institute of Software, Chinese Academy of Sciences, Beijing, China*
[7]*Joint Center for Quantum Information and Computer Science, University of Maryland, College Park, Maryland, USA*
[8]*Department of Physics and Astronomy, University of Waterloo, Waterloo, Ontario N2L 3G1, Canada*
[9]*Canadian Institute for Advanced Research, Toronto, Ontario, Canada*
[10]*Perimeter Institute for Theoretical Physics, Waterloo N2L 2Y5, Ontario, Canada*

Quantum state tomography via local measurements is an efficient tool for characterizing quantum states. However it requires that the original global state be uniquely determined (UD) by its local reduced density matrices (RDMs). In this work we demonstrate for the first time a class of states that are UD by their RDMs under the assumption that the global state is pure, but fail to be UD in the absence of that assumption. This discovery allows us to classify quantum states according to their UD properties, with the requirement that each class be treated distinctly in the practice of simplifying quantum state tomography. Additionally we experimentally test the feasibility and stability of performing quantum state tomography via the measurement of local RDMs for each class. These theoretical and experimental results demonstrate the advantages and possible pitfalls of quantum state tomography with local measurements.

Introduction—Quantum state tomography (QST) is one of the most famous double-edged swords in quantum information science. On the one hand, QST provides a complete description of an arbitrary quantum state, which is essential for benchmarking and validating quantum devices [1–5]. On the other hand, the exponential resources QST requires make scaling it to large systems infeasible in practice. In the past decade, tremendous effort has been devoted to boosting the efficiency of QST [6–12]. QST via reduced density matrices (RDMs) [13–18] is one especially promising approach, as it is significantly less resource-intensive and many experimental setups are able to perform local measurements conveniently and accurately. One criterion for adopting this approach is that the global state has to be the only state which is compatible with its RDMs, that is, it must be uniquely determined (UD) by its RDMs.

The UD criterion can be further classified into two categories: uniquely determined among all states (UDA) and uniquely determined among pure states (UDP) by local RDMs[1]. The quantum states of many physically realistic quantum systems usually belong to the UDA category. These systems involve only few-body interactions [24], and possess ground states which exhibit special properties [25–28]. To reconstruct states of this type, experimentalists need only measure RDMs and search for the global state which is compatible with these RDMs. This saves an exponential number of measurements [29].

In the case of states which satisfy the UDP criterion, two assumptions must be made if one wishes to reconstruct such states via RDMs. First, the experimentally prepared states must be (nearly) pure. Second, the search space of possible reconstructions must be limited to pure states, otherwise the searching procedure may return incorrect mixed states with the same RDMs. Despite these assumptions, searching for UDP states has the advantage of significantly reducing the number of search parameters since the search space is pure. Traditionally this has been the approach for dealing with many related problems, for instance, the famous Pauli problem and its finite dimensional versions [30, 31].

In this Letter, we resolve the relation between the UDP and UDA criteria and it is shown that there are states that is UDP but not UDA. Therefore, one should classify many-body quantum states into three different non-trivial classes: (A) neither UDP nor UDA; (B) UDA; (C) UDP but not UDA. One may argue that the existence of states of class (C) is trivial as the set of pure states is of a much lower dimension then that of the mixed states. We emphasize however this is not the case: when constructing examples of states of class (C), one is working with pure states that are already UDP, a strong restriction on the states under consideration, and the dimension argument does not work. In fact, to the contrary, it was known that for all three-qubit states, UDP equals UDA, and there are no states in class (C). It is indeed a surprise that, when considering four and more qubit systems, non-trivial examples emerge in class (C). In particular, we present a class of four-qubit states that are UDP by their two-particle RDMs (2-RDMs), but fail to be UDA. This is the first separation be-

[1] In this work, UD refers to UD by its RDMs unless otherwise specified. For the background of UD via general measurements, see appendix A in [19] for more details.

tween UDA and UDP in the setting of RDMs.

Our findings have important consequence to the RDM approach to state tomography, but are illuminating also to other areas of related research. First, the existence of states in class (C) must reveal interesting geometry of the many-body quantum state space. Our usual intuition about the state space looks more like the picture in Fig. 1(a)—the Bloch sphere. In this simple situation, one easily verifies that UDP equals UDA. However, in higher dimensional state spaces, projections of the state space could possibly look like Fig. 1(b), where UDP may not imply UDA. Second, the UDA versus UDP problem, originated from the study of ground state of local Hamiltonians, also sheds light on the structure of many-body entanglement as the local determination problem of entangled state is of fundamental importance.

Our construction is based on the study of 4-qubit symmetric ($i.e.$ bosonic) states. Note that the properties of bosonic states have recently been extensively studied theoretically [32–34] and experimentally [35, 36] due to their significant roles in characterizing cold atomic systems.

To illustrate the validity of our construction, we experimentally demonstrate the reconstruction of a series of 4-qubit states by measuring their 2-RDMs. We examine the differences among states of the three possible classes. We test the robustness (stability) against experimental errors of our construction.

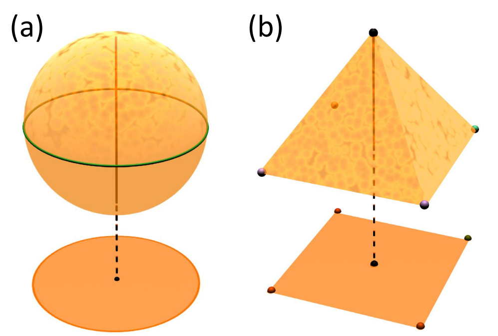

Figure 1. Three-dimensional caricatures of the possible shapes of state space, and the space of reduced density matrices as projections. Pure states are given by the extreme points. (a) A sphere, for which all boundary points are extreme points. Only the points on the boundary of the projected circle have a unique preimage in the state space, and so are UDA. All the interior points have multiple extreme points in their preimage, so they are not UDP. Thus UDP implies UDA. (b) A polytope, for which the five vertices are extreme points. The four corner points have a unique preimage in the state space, and so are UDA. However, one interior point located at the centre has multiple preimages where only one is an extreme point, so it is UDP but not UDA.

Three classes—We classify 4-qubit pure states into three classes according to how they are UD by their 2-RDMs, and present some examples for each class.

Class A: neither UDP nor UDA. Consider the GHZ-type state $\alpha|0000\rangle + \beta|1111\rangle$, whose 2-RDMs are

$$|\alpha|^2|00\rangle\langle 00| + |\beta|^2|11\rangle\langle 11|. \tag{1}$$

It is not UDP (thus not UDA) since any pure state $\alpha|0000\rangle + e^{i\phi}\beta|1111\rangle$ or mixed state $|\alpha|^2|0000\rangle\langle 0000| + |\beta|^2|1111\rangle\langle 1111|$ has the same 2-RDMs. Therefore, to reconstruct 4-qubit GHZ-type states experimentally, it is insufficient to only measure its 2-RDMs, even if assuming the prepared state is pure.

Class B: UDP and UDA. The W-type state

$$|\mathrm{W}\rangle = a|0001\rangle + b|0010\rangle + c|0100\rangle + d|1000\rangle, \tag{2}$$

is known to be UDA [37], and also UDP. Unlike the GHZ-type state, to reconstruct the global state, one needs only know its 2-RDMs.

Class C: UDP but not UDA. Existence of this type of states are the main theoretical results of this paper. Up until now, no such states are known. This is likely due to the fact that analytically determining the uniqueness properties of quantum states is notoriously difficult in general.

The outline of our approach is as follows. We focus on the 4-qubit bosonic (symmetric) state $|\psi_S\rangle = \sum_{j=0}^{4} c_j|w_j\rangle$, where the normalized Dicke state $|w_j\rangle$ is defined to be proportional to $P_{\text{sym}}\big(|0\rangle^{\otimes j} \otimes |1\rangle^{\otimes 4-j}\big)$ with P_{sym} being the projection onto the 4-qubit symmetric subspace. This symmetry assumption significantly simplifies the analysis since all the 2-RDMs are the same. To further simplify the analysis, we assume $c_1 = c_3 = 0$ and c_0, c_2 and c_4 are all real:

$$|\psi_S\rangle = c_0|w_0\rangle + c_2|w_2\rangle + c_4|w_4\rangle. \tag{3}$$

To determine the parameter regions of c_0, c_2, c_4 where $|\psi_S\rangle$ is UDP but not UDA, we take three steps:

Step 1. First we prove that there is no other pure bosonic state which has the same 2-RDMs as $|\psi_S\rangle$ when $|\psi_S\rangle$'s 2-RDMs have three distinct non-zero eigenvalues.

Step 2. Next we observe that any pure bosonic state which is uniquely determined among all other pure bosonic states is also UDP.

Step 3. Finally we provide the region where the 2-RDMs of $|\psi_S\rangle$ are separable. $|\psi_S\rangle$ is guaranteed not to be UDA in this region. Therefore, within this parameter region, $|\psi_S\rangle$ is UDP but not UDA as long as its 2-RDMs are non-degenerate and not rank one.

We direct the reader to appendix B for steps 1 and 2, and appendix C for step 3 in the Supplemental Material [19]. Note that for $|\psi_S\rangle$ in this class, all the mixed states which share the same RDMs with $|\psi_S\rangle$ form a convex set. This set ,with $|\psi_S\rangle$ as an extreme point, has infinite states.

Experiment—We experimentally inspect all three classes of state using nuclear magnetic resonance (NMR), and test their stability against experimental noise. The 4-qubit sample is ^{13}C-labeled trans-crotonic acid dissolved in d6-acetone, where the molecular structure and Hamiltonian form are shown in appendix E [19]. All experiments were carried out on a Bruker DRX 700MHz spectrometer at room temperature.

The experiments are divided into three steps: (i) prepare the initial state $|0000\rangle$; (ii) evolve $|0000\rangle$ to the desired state in each class; (iii) measure the final state by full QST and 2-RDMs, reconstruct the original state via the measured 2-RDMs, and compare it with the full QST result. We describe each step briefly as follows. For more experimental details, see appendices E and F in [19].

(i) In the majority of experiments in quantum information, $|0\rangle^{\otimes n}$ is chosen as the input state. In NMR we instead generate a so-called pseudo-pure state (PPS) from the thermal equilibrium state. This initialization step is realized by the spatial averaging technique [38–40], which involves both unitary and non-unitary (realized by z-gradient pulses) transformations. The form of 4-qubit PPS is

$$\rho_{0000} = \frac{1-\epsilon}{16}\mathbb{I} + \epsilon|0000\rangle\langle 0000|, \tag{4}$$

where $\mathbb{I}$ is identity and $\epsilon \approx 10^{-5}$ is the polarization. Although the PPS is highly mixed, the large $\mathbb{I}$ does not evolve under any unital propagator nor is it observed in NMR spectra. Hence, only the deviated part $|0000\rangle$ contributes to the experimental results and the PPS is able to serve as an input state.

(ii) The next step is to create the desired states of the different UD classes. The radio-frequency (RF) pulses during this procedure are optimized by the gradient ascent pulse engineering (GRAPE) algorithm [41, 42], and are designed to be robust to the static field distributions (T_2^* process) and RF inhomogeneity. The designed fidelity for each pulse exceeds 0.99, and all pulses are rectified via a feedback-control setup in the NMR spectrometer to minimize the discrepancies between the ideal and implemented pulses [43, 44].

Class A: States belonging to this class are neither UDP nor UDA by their 2-RDMs. The following states are in class A

$$\begin{aligned} |\mathrm{GHZ}\rangle_+ &= \alpha|0000\rangle + \beta|1111\rangle, \\ |\mathrm{GHZ}\rangle_- &= \alpha|0000\rangle - \beta|1111\rangle, \\ \rho^{\mathrm{G}}_{\mathrm{mix}} &= |\alpha|^2|0000\rangle\langle 0000| + |\beta|^2|1111\rangle\langle 1111|, \end{aligned} \tag{5}$$

and ρ^{G}_{+} and ρ^{G}_{-} are the density matrices of $|\mathrm{GHZ}\rangle_+$ and $|\mathrm{GHZ}\rangle_-$, respectively. All of these states have the same 2-RDMs, which means that the 2-RDMs are not sufficient to reconstruct these states. To verify this, we first need to prepare each state in Eq. (5) from $|0000\rangle$. For ρ^{G}_{+}, qubit 1 firstly undergoes a rotation around y-axis that $R_y(\theta) = e^{-i\theta\sigma_y/2}$ with $\theta = 2\arccos(\alpha)$. Then three controlled-NOT (CNOT) gates CNOT_{12}, CNOT_{13} and CNOT_{14} are applied consecutively, where qubit 1 is the control and others are targets. The single-qubit rotation $R_y(\theta)$ is realized by a 1 ms GRAPE pulse and the 3 CNOT gates are realized by a 30 ms GRAPE pulse. We can similarly construct ρ^{G}_{-} by instead employing a single-qubit rotation of $R_y(-\theta) = e^{i\theta\sigma_y/2}$. For $\rho^{\mathrm{G}}_{\mathrm{mix}}$, we simply prepare a classical distribution of two pure states $|0000\rangle$ and $|1111\rangle$. In these experiments we prepare nine distinct states by varying α from 0.1 to 0.9 with 0.1 increment.

Class B: States belonging to this class are both UDP and UDA, with the W-type state in Eq. (2) being a typical example. In experiment, we simply set $a = b$ and $c = d$, and then

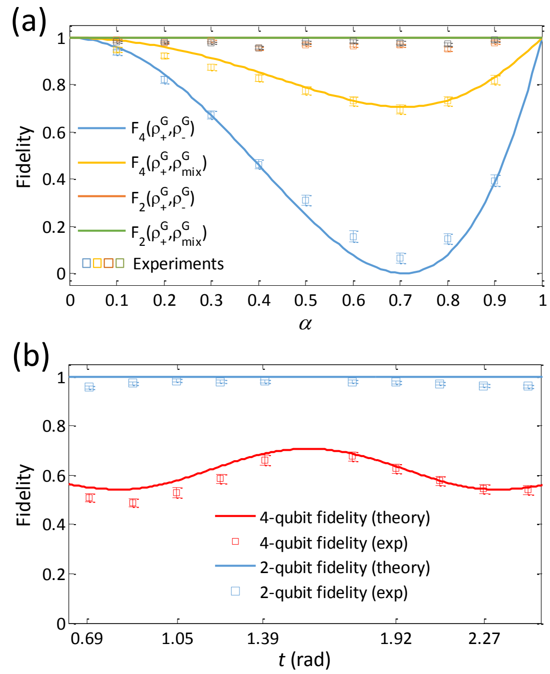

Figure 2. (a) GHZ-type states (Class A) such as ρ^{G}_{+} in Eq. (5) are neither UDP nor UDA. The 4-qubit fidelities between ρ^{G}_{+} and ρ^{G}_{-} (blue), and ρ^{G}_{+} and ρ^{G}_{mix} (yellow) are completely different, but they do have the same 2-RDMs (red and green, where the worst-case fidelity out of six possible 2-RDM fidelities is shown) up to minor experimental errors. The error bars are calculated from the imperfection of the GRAPE pulses and fitting procedure. (b) States in Class C are not UDA, so there can exist mixed states between which they have very low 4-qubit fidelity (red), but the same 2-RDMs (blue). However, these types of states are UDP so there do not exist any other 4-qubit pure states with the same 2-RDMs.

prepare six inputs $|\mathrm{W}\rangle$ by changing a from 0.1 to 0.6 with 0.1 increment. This state preparation is directly realized by a state-to-state GRAPE pulse with a duration of 20 ms.

Class C: States belonging to this class are UDP but not UDA. The type of state we prepare, $|\psi_S\rangle$ is described in Eq. (3) and conforms to the following parametrization

$$\begin{aligned} c_0 &= \frac{\sin t - \sin\theta\cos t}{\sqrt{2}}, \\ c_2 &= \cos\theta\cos t, \\ c_4 &= -\frac{\sin\theta\cos t + \sin t}{\sqrt{2}}, \end{aligned}$$

where we fix $\theta = \pi/12$ and choose t from $\pi/6 + \pi/18$ to $5\pi/6 - \pi/18$, and increment by $\pi/18$. With the exception of the point $t = \pi/2$ this curve lies within the region of states that are UDP but not UDA, as outlined in appendices A and B. All these states are prepared by state-to-state GRAPE pulses with a fixed duration of 20 ms. In order to demonstrate that these states are not UDA we also prepare corresponding mixed states with the same 2-RDMs as outlined in appendix D in [19].

(iii) After preparing these states, we perform 4-qubit QST [45, 46], which includes measuring the 2-RDMs. To determine the original 4-qubit state, a maximum likelihood approach [47] is adopted to reconstruct the most likely state based on the measured 2-RDMs.

Results—Now we discuss the effectiveness and stability of QST via 2-RDMs for each class of states.

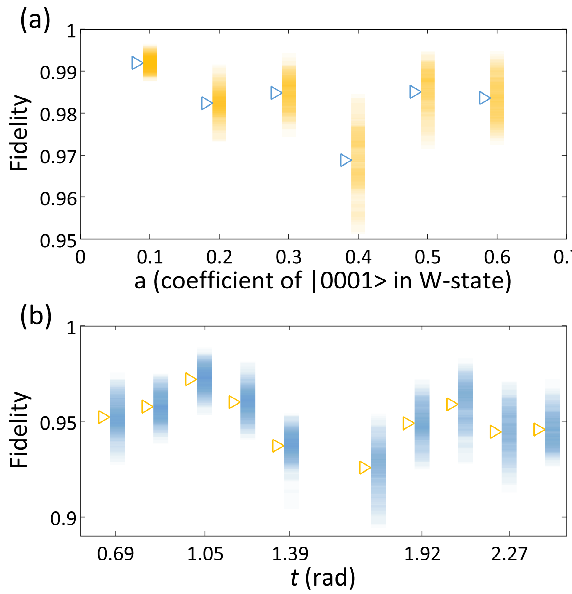

Figure 3. Stability test against experimental noise for $|\mathrm{W}\rangle$ and $|\psi_S\rangle$. The noise is artificially added in Gaussian distribution to the measured 2-RDMs under experimental conditions, by randomly sampling 90 distinct sets of 2-RDMs. The arrows indicate the mean for each sampled results. (a) Fidelities of the $|\mathrm{W}\rangle$ (Class B) in noisy environment. The x-axis is the coefficient a defined in Eq. (2). (b) Fidelities of the $|\psi_S\rangle$ (Class C) in noisy environment, as a function of t defined in Eq. (3).

Class A: In Fig. 2(a), it is clear that any two of ρ_+^{G}, ρ_-^{G} and ρ_{mix}^{G} have completely different fidelities in the 4-qubit form (blue and yellow), but they share the same 2-RDMs up to minor experimental errors (red and green). Therefore these states are neither UDP nor UDA, and it is insufficient to rely only on their 2-RDMs for QST.

Class B: The W-type state in Eq. (2) is known to be UDA. In Fig. 3(a), the blue triangles represent the fidelities $F(\rho_{\text{qst}}^{\mathrm{W}}, \rho_{\text{2rdm}}^{\mathrm{W}})$ between the prepared 4-qubit state $\rho_{\text{qst}}^{\mathrm{W}}$ via full QST and the reconstructed 4-qubit state $\rho_{\text{2rdm}}^{\mathrm{W}}$ via 2-RDMs. For every tested W-type state, the worst fidelity is still about 97% as shown by the triangles in Fig. 3(a). This indicates that the 2-RDMs are indeed sufficient for the reconstruction of the original 4-qubit state.

However, under realistic experimental conditions, the prepared state $\rho_{\text{qst}}^{\mathrm{W}}$ unavoidably deviates from the desired state. This may drive it outside the UDA region, so that it is no longer UDA. To test if this is the case, we simulate different outputs of 2-RDMs by adding Gaussian distributed noise and repeating the reconstruction of the 4-qubit state via the 2-RDMs, as outlined in appendix F in [19]. From the yellow bars in Fig. 3(a) it can be seen that even with artificial noise, QST via 2-RDMs is stable, since the fidelity is always over 0.95.

Class C: This class is UDP, which means we do not have any other pure state that gives the same 2-RDMs other than the target state. However, it is not UDA, so there do exist some mixed state (see appendix D in [19]) with the same 2-RDMs. Fig. 2(b) illustrates such results. Both in theory and experiment, we see that the target state $|\psi_S\rangle$ and a corresponding mixed state have low fidelity with one another (yellow), but the same 2-RDMs (blue). Therefore, when reconstructing this type of 4-qubit state via its 2-RDMs, we need to assume that the original state is pure. Otherwise it is likely to obtain some mixed state which will not necessarily be the true state of the system.

Similarly to the W-type state, we test whether the UDP property of $|\psi_S\rangle$ is stable against noise. As seen in Fig. 3(b), even under the application of Gaussian noise, as long as we assume our state is pure we can always reconstruct the correct 4-qubit state with high fidelity (>0.90) using only its 2-RDMs.

Conclusion—In summary, we disprove the hypothesis that UDP implies UDA for RDMs [16] by demonstrating the existence of a family of 4-qubit states that are UDP but not UDA by their 2-RDMs. This new finding allows us to classify pure states into three classes according to their UD properties, in order to improve the efficiency of QST: in Class A where the state is neither UDP nor UDA, full QST is necessary; in Class B where the state is UDP and UDA, the measurement of 2-RDMs is sufficient to determine the global state; in Class C where the state is UDP but not UDA, the measurement of 2-RDMs combined with the assumption that the global state is pure is sufficient. This approach simplifies QST significantly, since full QST of n qubits requires $4^n - 1$ observables while 2-RDM measurement requires $\binom{n}{1} \times 3 + \binom{n}{2} \times 9$ observables (all weight-1 and weight-2 Pauli operators) only.

We check the feasibility of this protocol for each class with a 4-qubit NMR quantum processor. The results indicate that for Classes B and C it is not necessary to implement the full QST—2-RDMs already enables the reproduction of the global state with high fidelities. As there are always experimental errors, we also demonstrate the stabilities of this protocol, namely, whether it is robust against experimental noise. The results reveal that the approach of doing QST solely via the measurement of 2-RDMs is robust to the noise under our experimental conditions, and hopefully behaves the same in other experimental platforms.

Acknowledgments. We thank Aharon Brodutch for his comments on the previous version of this paper. We are grateful to the following funding sources: NSERC (D.L., N.Y., J.K., B.Z. and R.L.); Industry Canada (R.L.); CIFAR (B.Z. and R.L.); the Department of Defense (J.C.); National Natural Science Foundation of China under Grants No. 11175094 and No. 91221205 (T.X. and G.L.); National Basic Research Program of China under Grant No. 2015CB921002 (T.X. and G.L.). T.X, D.L, J.K and N.Y contributed equally to this work.

* n5yu@uwaterloo.ca
† zengb@uoguelph.ca

[1] G. M. D'Ariano, M. De Laurentis, M. G. Paris, A. Porzio, and S. Solimeno, J. Opt. B: Quantum Semiclass. Opt. **4**, S127 (2002).
[2] H. Häffner, W. Hänsel, C. Roos, J. Benhelm, M. Chwalla, T. Körber, U. Rapol, M. Riebe, P. Schmidt, C. Becher, *et al.*, Nature **438**, 643 (2005).
[3] D. Leibfried, E. Knill, S. Seidelin, J. Britton, R. B. Blakestad, J. Chiaverini, D. B. Hume, W. M. Itano, J. D. Jost, C. Langer, *et al.*, Nature **438**, 639 (2005).
[4] A. I. Lvovsky and M. G. Raymer, Rev. Mod. Phys. **81**, 299 (2009).
[5] M. Baur, A. Fedorov, L. Steffen, S. Filipp, M. P. da Silva, and A. Wallraff, Phys. Rev. Lett. **108**, 040502 (2012).
[6] H. Kosaka, T. Inagaki, Y. Rikitake, H. Imamura, Y. Mitsumori, and K. Edamatsu, Nature **457**, 702 (2009).
[7] M. Vanner, J. Hofer, G. Cole, and M. Aspelmeyer, Nat. Commun. **4** (2013).
[8] S. T. Flammia, D. Gross, Y.-K. Liu, and J. Eisert, New J. Phys. **14**, 095022 (2012).
[9] D. Gross, Y.-K. Liu, S. T. Flammia, S. Becker, and J. Eisert, Phys. Rev. Lett. **105**, 150401 (2010).
[10] D. Lu, T. Xin, N. Yu, Z. Ji, J. Chen, G. Long, J. Baugh, X. Peng, B. Zeng, and R. Laflamme, Phys. Rev. Lett. **116**, 230501 (2016).
[11] C. H. Baldwin, I. H. Deutsch, and A. Kalev, Phys. Rev. A **93**, 052105.
[12] J. Haah, A. W. Harrow, Z. Ji, X. Wu, and N. Yu, Proceedings of the 48th Annual ACM Symposium on Theory of Computing , 913 (2016).
[13] N. Linden, S. Popescu, and W. K. Wootters, Phys. Rev. Lett. **89**, 207901 (2002).
[14] N. Linden and W. K. Wootters, Phys. Rev. Lett. **89**, 277906 (2002).
[15] L. Diósi, Phys. Rev. A **70**, 010302 (2004).
[16] J. Chen, Z. Ji, M. B. Ruskai, B. Zeng, and D.-L. Zhou, J. Math. Phys. **53**, 072203 (2012).
[17] J. Chen, Z. Ji, B. Zeng, and D. L. Zhou, Phys. Rev. A **86**, 022339 (2012).
[18] J. Chen, H. Dawkins, Z. Ji, N. Johnston, D. Kribs, F. Shultz, and B. Zeng, Phys. Rev. A **88**, 012109 (2013).
[19] See supplemental material for details, which includes Refs. [20–23].
[20] M. A. Nielsen and I. L. Chuang, *Quantum computation and quantum information* (Cambridge university press, 2010).
[21] T. Heinosaari, L. Mazzarella, and M. M. Wolf, Commun. Math. Phys. **318**, 355 (2013).
[22] M. Horodecki, P. Horodecki, and R. Horodecki, Phys. Lett. A **223**, 1 (1996).
[23] N. S. Jones and N. Linden, Phys. Rev. A **71**, 012324 (2005).
[24] M. B. Hastings, arXiv:1008.5137 (2010).
[25] M. M. Wolf, F. Verstraete, M. B. Hastings, and J. I. Cirac, Phys. Rev. Lett. **100**, 070502 (2008).
[26] D. Perez-Garcia, F. Verstraete, M. M. Wolf, and J. I. Cirac, Quantum Inf. Comput. **7**, 401 (20067).
[27] F. Verstraete, V. Murg, and J. I. Cirac, Adv. Phys. **57**, 143 (2008).
[28] J. I. Cirac and F. Verstraete, J. Phys. A **42**, 504004 (2009).
[29] M. Cramer, M. B. Plenio, S. T. Flammia, R. Somma, D. Gross, S. D. Bartlett, O. Landon-Cardinal, D. Poulin, and Y.-K. Liu, Nat. Commun. **1**, 149 (2010).
[30] W. Pauli, *Die allgemeinen prinzipien der wellenmechanik* (Springer Berlin, 1958).
[31] S. Weigert, Phys. Rev. A **45**, 7688 (1992).
[32] K. Eckert, J. Schliemann, D. Bruss, and M. Lewenstein, Ann. Phys. **299**, 88 (2002).
[33] T. Bastin, S. Krins, P. Mathonet, M. Godefroid, L. Lamata, and E. Solano, Phys. Rev. Lett. **103**, 070503 (2009).
[34] N. Yu, C. Guo, and R. Duan, Phys. Rev. Lett. **112**, 160401 (2014).
[35] M. Cramer, A. Bernard, N. Fabbri, L. Fallani, C. Fort, S. Rosi, F. Caruso, M. Inguscio, and M. Plenio, Nat. Commun. **4**, 2161 (2013).
[36] R. McConnell, H. Zhang, J. Hu, S. Cuk, and V. Vuletic, Nature **519**, 439 (2015).
[37] P. Parashar and S. Rana, Phys. Rev. A **80**, 012319 (2009).
[38] D. G. Cory, A. F. Fahmy, and T. F. Havel, Proc. Natl. Acad. Sci. **94**, 1634 (1997).
[39] D. Lu, N. Xu, R. Xu, H. Chen, J. Gong, X. Peng, and J. Du, Phys. Rev. Lett. **107**, 020501 (2011).
[40] T. Xin, H. Li, B.-X. Wang, and G.-L. Long, Phys. Rev. A **92**, 022126 (2015).
[41] N. Khaneja, T. Reiss, C. Kehlet, T. Schulte-Herbrüggen, and S. J. Glaser, J. Magn. Reson. **172**, 296 (2005).
[42] C. A. Ryan, C. Negrevergne, M. Laforest, E. Knill, and R. Laflamme, Phys. Rev. A **78**, 012328 (2008).
[43] O. Moussa, M. P. da Silva, C. A. Ryan, and R. Laflamme, Phys. Rev. Lett. **109**, 070504 (2012).
[44] D. Lu, H. Li, D.-A. Trottier, J. Li, A. Brodutch, A. P. Krismanich, A. Ghavami, G. I. Dmitrienko, G. Long, J. Baugh, *et al.*, Phys. Rev. Lett. **114**, 140505 (2015).
[45] G. M. Leskowitz and L. J. Mueller, Phys. Rev. A **69**, 052302 (2004).
[46] J.-S. Lee, Phys. Lett. A **305**, 349 (2002).
[47] J. B. Altepeter, E. R. Jeffrey, and P. G. Kwiat, Adv. At. Mol. Opt. Phy. **52**, 105 (2005).